A multiscale approach simulating generic pool boiling

Höhne, T.; Lucas, D.;

Originally published:

May 2020

Nuclear Science and Engineering 194(2020)10, 859-872

DOI: https://doi.org/10.1080/00295639.2020.1764265

A multi-scale approach simulating generic pool boiling

T. Höhne, D. Lucas

Helmholtz-Zentrum Dresden-Rossendorf (HZDR) - Institute of Fluid Dynamics

Bautzner Landstraße 400, D-01328 Dresden, Germany

ABSTRACT

The paper presents an application of the GENTOP model for phase transfer and discusses the sub-models used. Boiling of a heated surface under atmospheric conditions is simulated by the multi-field CFD approach. Sub-cooled water in a generic pool is heated up first in the near wall region leading to the generation of small bubbles. Further away from the bottom wall larger bubbles are generated by coalescence and evaporation. The CFD simulation bases on the recently developed GEneralized TwO Phase flow (GENTOP) concept. It is a multi-field model using the Euler-Euler approach and it allows the consideration of different local flow morphologies including transitions between them. Small steam bubbles are handled as dispersed phases while the interface of large gas structures is statistically resolved. The GENTOP sub-models need a constant improvement and separate, intensive validation effort using CFD grade experiments.

KEYWORDS

multi-phase, boiling, GENTOP, multi-scale, CFD

I. INTRODUCTION

Due to latent heat, boiling heat transfer plays a very important role in wide number of applications in many technological and industrial areas including nuclear reactor cooling systems, car cooling and refrigeration systems. Boiling is a process in which heat transfer causes liquid evaporation. It can be classified as saturated boiling and subcooled boiling. In the saturated boiling, the bulk temperature of the fluid is as equal as its saturation temperature, in the subcooled boiling regime the bulk temperature of the fluid is less than its saturation temperature. When a liquid is in contact with a surface maintained at a temperature above the saturation temperature of the liquid, boiling will eventually occur at that liquid-solid interface. Conventionally, based on the relative bulk motion of the body of a liquid to the heating surface, the boiling is divided into

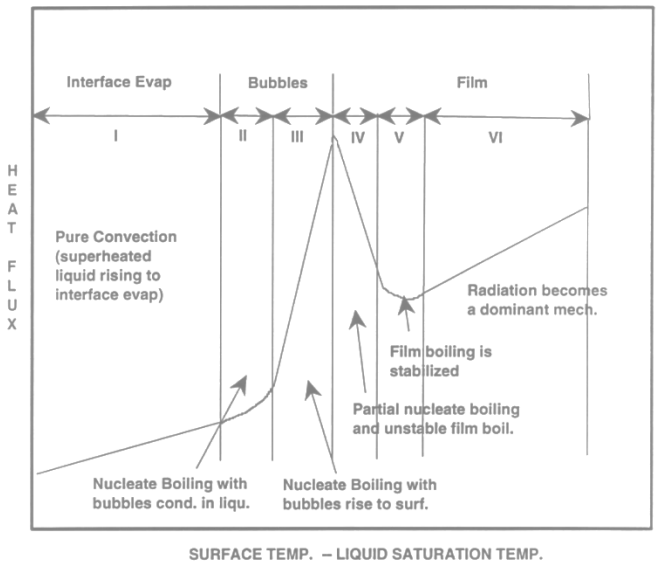

Figure 1: Physical Interpretation of Boiling Curve (Farber, [2])

two categories; pool boiling and convective boiling. Pool boiling is the process in which the heating surface is submerged in a large body of stagnant liquid. The relative motion of the vapor produced and the surrounding liquid near the heating surface is due primarily to the buoyancy effect of the vapor. Nevertheless, the body of the liquid as a whole is essentially at rest. The extensive study on the effect of the difference in the temperature of the heating surface and the liquid, ΔT, was first done by Nukiyama [1]. However, it was the experiment by Farber and Scorah [2] that gave the complete picture of the heat transfer rate in the pool boiling process as a function of ΔT. Applying the Newton's law of cooling, $q'' = h\Delta T$, the heat transfer coefficient, h, was used to characterize the pool boiling process over a range of ΔT as illustrated by the boiling curve in Figure 1. Also Figure 2 shows the stages of pool boiling according to Kreith and Bohn, 1993 [3]. When the excess temperature lies between 0.2 and 4 degrees Celsius, only free convection can be observed. When excess temperature is between 4 and 20 degrees there is nucleate boiling. In this region isolated bubbles and or columns or slugs of bubbles will exist. In this region, the heat transfer coefficient starts to decrease due to increased bubbles, which lessen the total surface-liquid contact. However, the heat transfer rate continues to increase because of the rising excess temperature until where the maximum heat transfer is reached. After this point the decrease in the coefficient surpasses the increase in excess temperature and the heat transfer rate begins to decrease. Between is the transition region between nucleate and film boiling. In this region there is a combination of both types of boiling. Because the surface is now primarily in contact with a combination of bubbles and a vapor film, the heat transfer coefficient is reduced drastically; and therefore, the heat transfer rate will continue to decrease. From there is only film boiling where the surface is covered by a vapor blanket. In this region there is no longer any surface to liquid contact; however, the heat transfer rate continues to increase as excess temperature increases because heat transfer by radiation becomes significant.

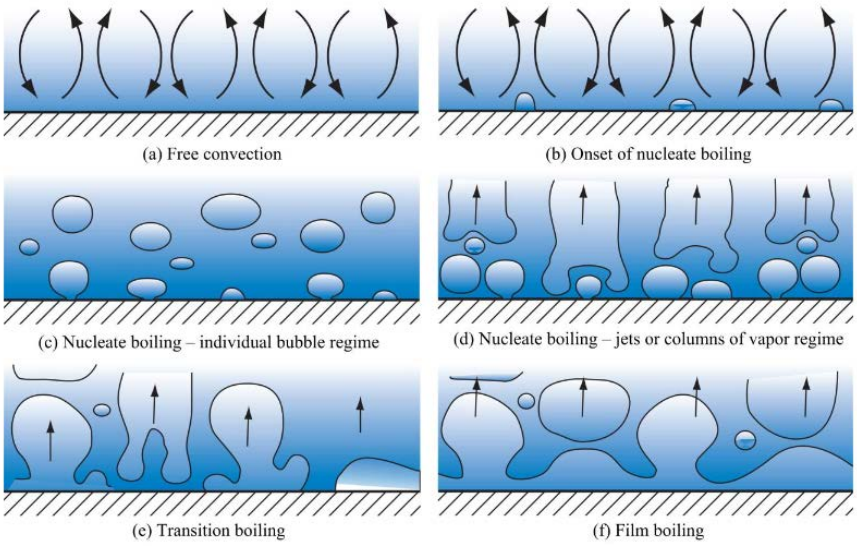

Figure 2: Four regimes of pool boiling in water at 1 atm. (www.engr.iupui.edu, Kreith and Bohn, 1993 [3])

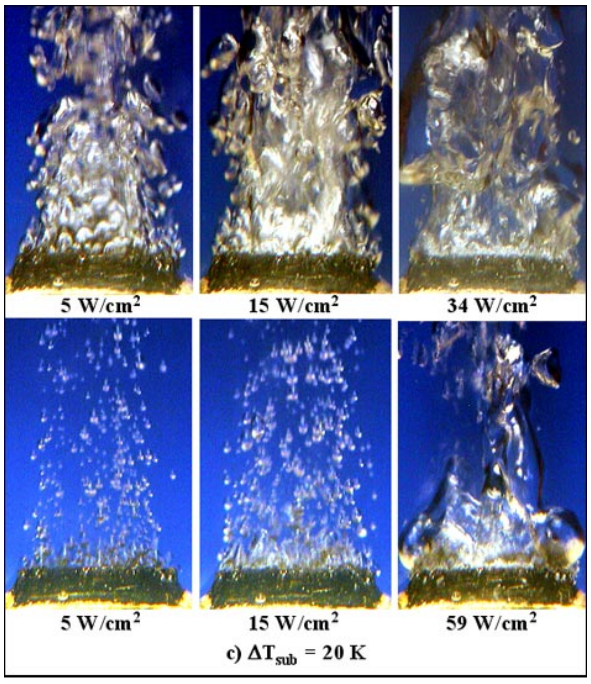

Figure 3: Pool boiling experiment at the ISNPS-UNM Test Facility [7]

Much progress has been achieved in establishing models to describe various multiphase boiling flow phenomena using Computational Fluid Dynamics (CFD). The GENTOP-concept [4] enables to consider such processes. The potential of this concept was demonstrated in Hänsch et al. [5,6] for

adiabatic flows and in Höhne et al. [4] with heat and mass transfer. In this paper the GENTOP concept is applied to simulate boiling effects in a pool where transitions from small bubbly flow to larger bubbles and structures are involved.

To show pictures from experiments for a better understanding of the boiling process in Figure 3 the experimental pool boiling facility at the Institute for Space and Nuclear Power Studies is used. The experiments were dedicated to investigating immersion cooling with dielectric liquids on porous graphite and finned surfaces with the application toward electronics cooling applications [7]. Systematic investigations were carried out using different boiling flat and finned surfaces (copper and porous graphite), at different liquid subcoolings (0° K = ΔTsub = 30° K), and at different surface orientations.

Thus, in order to fully understand and predict the boiling phenomenon, the high gas volume fractions must be taken into account. Realizing this need, the GENTOP concept was utilized and further developed for flows with heat and mass transfer [4]. It allows the modelling for bubbles smaller than the grid size and tracking the interface of large continuous bubbles (larger than the grid size). Thus, it is like a combination of Euler –Euler two fluid modeling and interface tracking techniques. It has been further advanced and validated for churn turbulent flow regimes (Montoya, [8]). This work presents a simulation of a generic pool boiling phenomenon with the help of the GENTOP concept in ANSYS-CFX, where important new models have been discussed and applied.

II. CFD SIMULATION OF GAS-LIQUID TWO PHASE FLOWS

II.A The generalized two phase flow (GENTOP) concept

GENTOP is based on a multi-field two-fluid approach. The flow is represented by a continuous liquid phase l, one or several poly-dispersed gas phases GasD and a continuous gas phase GasC.

The dispersed gas GasD is modelled in the framework of the inhomogeneous Multiple Size Group (iMUSIG) -approach to deal with different bubble size groups and associated velocity fields (Krepper et al. [9]). Within the poly-dispersed gas phases, transfers between different bubble size groups due to coalescence- and breakup as well as due to condensation and evaporation are taken into account by appropriate models.

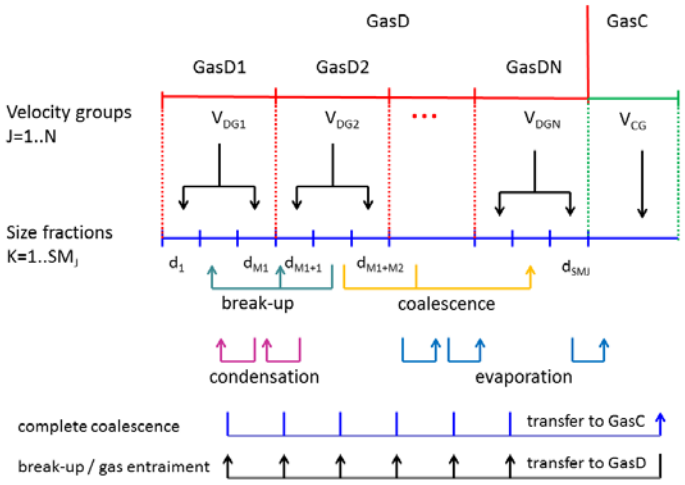

Figure 4: Scheme of the extended GENTOP model [4] including phase transfer

GENTOP has been developed as an extension of the inhomogeneous MUltiple SIze Group (iMUSIG) by adding a potentially continuous gas phase GasC which is included within the MUSIG framework. (Figure 4). This last velocity group represents all gas structures which are larger than an equivalent spherical bubble diameter, d(dg,max). The interactions between GasC and the liquid phase are handled in a similar way like in the AIAD-concept (Höhne et al. [10]). This includes the blending for bubbly flow, interface and droplet regions allowing to apply e.g. for a low volume fraction of GasC closures for bubbly flow. For this reason it is called potentially continuous phase.

II.B Turbulence modeling

In terms of turbulence treatment, the dispersed phase zero equation is used for the dispersed gaseous phases, while the SST *k-ω* approach is used for the liquid phase. One of the advantages of the *k-ω* model over the *k-ε* is the treatment when in low Reynolds numbers for a position close to the wall. The effect of bubbles on the liquid turbulence is considered by additional source terms (Rzehak and Krepper, [8]).

II.C Modeling of momentum transfer between the dispersed phases and liquid

Due to the averaging of the conservation equations all information on the interface is lost, but has to be reintroduced by the use of closure relations. The closure laws objective is to account for the mass and momentum transfer between the different fields and phases while providing the functional form expected from the interfacial forces. The present models are limited by the need of local condition dependent coefficients, derived from the fact that the closure laws have been developed for ideal bubbly flow and are now being applied to churn-turbulent flow and slug conditions.

Rzehak et al. [11] have tested and successfully validated a number of poly-dispersed closure laws for Euler-Euler calculations and set up a so called Baseline Model for multiphase poly-dispersed bubbly flows (Table 1).

The total momentum exchange between dispersed gas and continuous liquid phase can be expressed as the superposition of several component forces (see Eq. 1).

$$\mathbf{M}_k^i = \mathbf{M}_k^D + \mathbf{M}_k^{VM} + \mathbf{M}_k^{TD} + \mathbf{M}_k^L + \mathbf{M}_k^W \tag{1}$$

In the baseline model (Rzehak et al. [12]) the drag force $\mathbf{M}_k^D$ is calculated according to Ishii and Zuber [13].

Table 1: Baseline model (Rzehak et al. [10]) for poly-dispersed flows used in GENTOP

Model	**Name**
Drag coefficient ($C_{D,k}$),	Ishii and Zuber [13]
Interfacial lift force	Tomiyama [14]
Turbulent dispersion force	Burns [15]
Wall lubrication force	Hosokawa [16]
Virtual mass	0.5

II.D Handling of the potentially continuous phase GasC

II.D.1 Interface detection

To resolve the interface of continuous gas structures, the interface has to be localized. This is based on an appropriate blending function Ψ_{surf} (Höhne et al. [4]). It bases on the volume fraction and its gradient and is designed in a generalized form capable for later applications describing not only bubble regions but also droplet regions. It replaces the blending taken from the AIAD model (Höhne, [10]) which was combined with a volume fraction based interface function in the original GENTOP concept of Hänsch et al. [5].

The interface blending function is defined as

$$\psi_{FS} = \varphi_{sf}\left(f_b - f_d\right) \tag{2}$$

which is equal to zero for at a interphase boundary. Additionally, it provides information about the morphology:

$$\psi_{FS} = \begin{cases} 1 & \text{bubble region} \\ 0 & \text{interface} \\ -1 & \text{droplet region} \end{cases}$$

In the recent application only the bubble region and the interface region are of interest. The blending functions for the potentially continuous-phase bubble regime f_b and droplet regime f_d are given by:

$$f_b = \frac{1}{2}\left[1+\cos\left(\pi\frac{\tilde{\alpha}^G - \left(\alpha_{b,crit} - \Delta_\alpha\right)}{2\Delta_\alpha}\right)\right] \tag{3}$$

$$f_d = \frac{1}{2}\left[1+\cos\left(\pi\frac{\tilde{\alpha}^L - \left(\alpha_{d,crit} - \Delta_\alpha\right)}{2\Delta_\alpha}\right)\right] \tag{4}$$

The interface blending function is given by:

$$\varphi_{sf} = \frac{1}{2}\left[1+\cos\left(\pi\frac{\nabla\tilde{\alpha}^c - \left(\nabla\alpha_{crit} - \Delta_{\nabla\alpha}\right)}{2\Delta_{\nabla\alpha}}\right)\right] \tag{5}$$

II.E Complete coalescence

During the calculation low fractions of dispersed gas in the region of mainly continuous gas might arise. To solve this unphysical situation a special coalescence method for complete gaseous mass transfer was established and is now included in the concept in order to replace the coalescence when the critical void fraction is reached. The coalescence rate is transferring the remained dispersed gas within a specific grid cell into continuous gas. The complete coalescence is turned off inside the interface in order to allow coalescence and breakup at those positions. The mass transfer is defined by:

$$S_{dg\to cg} = \max(-\Psi_{surf}, 0)\,\rho_{dg}\alpha_{dg} / \tau_{dg\to cg} \tag{6}$$

where $\tau_{dg\to cg} = \Delta t$ is a time constant that regulates how fast the mechanism occurs in consistency with the numerical scheme.

II.F Clustering force

The clustering force (Figure 5) allows the transition from the dispersed towards the continuous gas phases using an aggregative effect within the volume fraction of the continuous gas. Modeling using an Eulerian approach will produce smearing of the volume fraction by numerical diffusion, thus this force produces interface stabilizing effects.

This force is the additional interfacial force acting exclusively between the continuous gas and the liquid phase and is included in the interfacial momentum transfer. This force acts proportionally to the gradient of the volume fraction of the liquid as given in the following eq. (7) with

$$M_{cg}^{clust} = -c_{clust}\max(\psi_{clust}, 0)\,\varphi_{clust}\,\rho_l\nabla\alpha_l \tag{7}$$

As soon as the specific critical void fraction of continuous gas is reached, this force will create regions of continuous gas volume fraction by inducing aggregation on the continuous gas phase volume fraction until a complete formation of gas structure is reached. The force acts outside the interface region, agglomerating the gas, and blends out as soon as the critical gradient of volume fraction appears, completely disappearing as a fully formed interface occurs$\left(\Psi_{surf} = 0\right)$. The clustering force

disappears within the continuous structure. A constant value of $c_{clust} = 1$ is recommended for the GENTOP application.

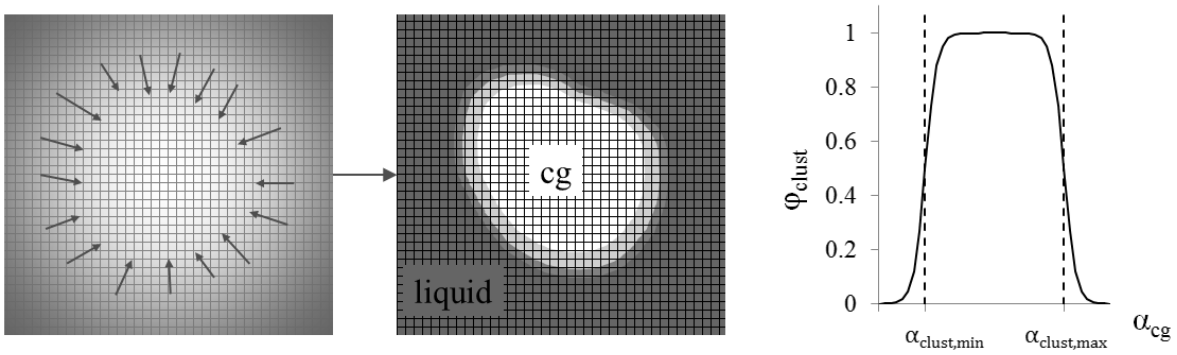

Figure 5: Detail of a continuous gas liquid interface, and the blending function for a filtered interface (from Hänsch et al. [5])

II.G Interfacial momentum transfer

The Algebraic Interfacial Area Density (AIAD) model, shown in Höhne et al. [10], allows detection of morphological form of two phase flow and is able to distinguish between bubbles, droplets and the interface through a corresponding switching via a blending function of each correlation from one object pair to another.

Based on Ψ_{surf} (blending function), formulations for interfacial area density and drag are defined as in eqs. (8) and (9),

$$A_{GasC} = (1-|\Psi_{surf}|)\, A_{fs} + a_{sign}|\Psi_{surf}|\, A_b + (1-a_{sign})|\Psi_{surf}|A_d \tag{8}$$

$$C_{D,GasC} = (1-|\Psi_{surf}|)\, C_{D,fs} + a_{sign}|\Psi_{surf}|\, C_{D,b} + (1-a_{sign})|\Psi_{surf}|C_{D,d} \tag{9}$$

II.H Phase change model for GasD and GasC

For the simulation of boiling, the thermal phase change model has been used for the disperse gas phase (GasD) and liquid pair and the continuous gas phase (GasC) and liquid pair.

In our case of heat transfer between liquid and gas, the use of overall heat transfer coefficient is not sufficient to model the interphase heat transfer process. This model considers separate heat transfer process on each side of the phase interface. This is achieved by using two heat transfer coefficients defined on each side of the phase interface.

The heat flux to liquid from the interface is given as:

$$q_l = h_l(T_s - T_l) \tag{10}$$

Similarly, the heat flux to gas from the interface:

$$q_g = h_g(T_s - T_g) \tag{11}$$

For spherical bubbles the Ranz Marshall correlation can be applied to calculate the Nusselt number. In the present simulation the Ranz Marshall [17] correlation was used for the disperse gas phase (GasD) and liquid pair. The Hughes and Duffey [18] model uses the surface renewal theory and is applied for the potentially continuous gas phase (GasC) and liquid pair.

The wall boiling model is only activated for the disperse gas phase (GasD) and liquid pair. Initially, water is below its saturation temperature. Water becomes supersaturated locally, leading to the

formation of bubbles. The bubbles will start departing and before the formation of next bubble, some of the heat will superheating the water. This process is known as quenching. In regions of the wall not affected by bubble growth, wall heat transfer to the water is described by single phase convective heat transfer. In the actual paper the wall boiling heat flux partitioning model developed at RPI (Kurul [19]) is applied. A detailed discussion of the aspects of wall boiling can be found in Krepper et al. [20]. However, a bubble dynamics model inside the heat partitioning approach has been developed and will be applied in GENTOP in future [21]. The bubble dynamics model is able to show the dependency of bubble departure diameter (lift off diameter) and frequency on the different physical quantities such as heat flux, liquid properties, sub-cooling temperature, design of channel (diameter, length) and mass flow rate. The implementation of this bubble dynamics model requires an update of the conventional nucleation site activation and heat partitioning in the GENTOP model. The new activation approach considers a distribution of cavity sizes and their influence on the activation temperature.

III. DEMONSTRATION CASE OF A WALL HEATED POOL

To illustrate the previous described concept a demonstration example of a wall heated pool is given. The pool has a length of 250 mm, a width of 100 mm and a height of 100 mm. Liquid water is considered at a pressure of 1 bar. At this pressure the saturation temperature amounts to 372 K. The initial temperature was set to a subcooling of 2 K. The temperature of the heated wall is set to a superheating of 38 K.

III.A Geometry, mesh and general setup

The pool is presented by a fully 3D geometry shown in Figure 6 along with the name of the different areas (i.e., hot wall at the bottom and degassing boundary on the top). The resulting mesh is made of approximately 326,000 hexahedral cells. A grid resolution study was conducted to ensure that convergence with respect to the spatial resolution has been achieved. A multiphase simulation was set up. Gas was described in the inhomogeneous poly-dispersed multiple size group (iMUSIG) framework by the dispersed gaseous phases GasD1 and GasD2 and the continuous gas phase GasC.

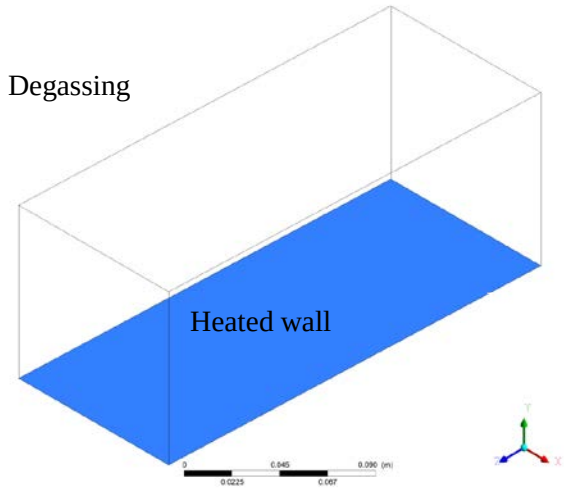

Figure 6: Pool Geometry

A total of four velocity fields, three for the gas and one for the continuous liquid were solved. Gas was assumed at saturation temperature.

Properties of dry steam at saturation temperature have been taken from steam tables. At the hot wall a wall boiling model generating GasD was applied. GasC then arise either by coalescence of GasD or by evaporation in the bulk.

Table 2: Solver setup

Advection scheme	**Option**	**High Resolution**
Transient scheme	Option Δt	Second order backward Euler 0.001 s
Convergence control	Timescale control Min./max. coeff. loops	Coefficient loops 4/50
Convergence criteria	Residual type Residual target	RMS 1e-04

For the heat and mass transfer between gas and liquid in the bulk the implemented phase change models using the Ranz-Marshall correlation [17] for the pair GasD/Liquid and the Hughes and Duffey [18] model for the potentially continuous gas phase (GasC) and liquid pair were applied. Table 2 shows the numerical scheme used in the case.

III.B Overview of the settings and models used in the GENTOP framework

The critical bubble diameter were the lift coefficient changes its sign is found at d_B = 5.4 mm. For GasD (dispersed gas) the iMUSIG model with three size fractions for GasD1 and three size fractions for GasD2 was applied. In this way the lift coefficient for GasD1 is clear different from the lift coefficient of GasD2. GasC was considered as the last size fraction of the iMUSIG framework. This allows to including it in the coalescence and fragmentation process. All gas structures equal or larger than 15 mm sphere equivalent diameter were assigned to GasC.

The coalescence and breakup models according to Luo & Svendsen [22] and Prince & Blanche [23] with coefficients of F_B=0.01 and F_C=2 were applied.

The momentum exchange between GasD and the liquid phase was simulated considering all exchange terms for drag and non-drag forces according to the baseline model for polydispersed flows [12] were used. Concerning the drag between GasC and Liquid the AIAD formulation was applied (Höhne [10]). The liquid phase was simulated using the shear stress transport (SST) turbulence model. The influence of bubbles of GasD on the liquid turbulence was considered. The exchange models were implemented using subdomains. Surface tension for the pair GasC and Liquid was implemented. Effects of numerical diffusion were compensated by an additional force acting between GasC and Liquid to keep the interface between GasC and Liquid stable (Clustering force).

The disappearance of unphysical fractions of dispersed gas in zones of prevailing GasC was enforced by complete coalescence. Concerning the turbulence of the liquid at the presence of an interface to GasC experiences with the AIAD model were used. Turbulence damping at the interface was considered and waves smaller than the grid resolution were treated as in the AIAD model [10].

IV. RESULTS AND DISCUSSION

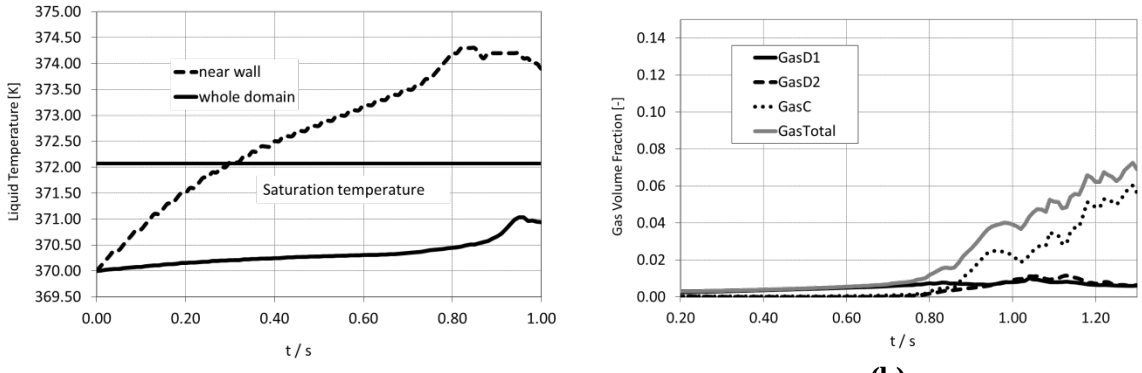

(a) **(b)**

Figure 7: Time course of the averaged near wall/whole domain liquid temperature (a) and the near wall volume fractions for the dispersed and continuous gas (b)

Figure 7 shows the time course of volume averaged parameters in the near wall region (averaging over a layer parallel to the wall with a cell thickness, 1 mm away from the wall) of the pool. The near wall temperature (Figure 7a) is rising from below saturation temperature (370 K) to 2.5 K above saturation. Afterwards the near wall temperature goes down to 2 K above saturation. During the first 0.8 s only dispersed gas GasD1 is generated by boiling (see Figure 7b). After this time GasD2 is generated due to boiling and coalescence and also continuous gas GasC arises, produced by coalescence of dispersed gas and direct bulk boiling.

In Figure 8 the cross sectional averaged values of liquid temperature (a) and the liquid superficial velocity (b) dependent on the height of the pool are shown. Figure 8 also presents gas volume fractions for dispersed gas (GasD1 and GasD2) and continuous gas (GasC) after a heating time of 0.5s (Figure 8c) resp. 1.0s (Figure 8d). In Figure 8a one can see the temperature rise during the heat up process of the water near the heated wall. There is an increase in the liquid superficial velocity (Figure 8b) during the boiling process, caused by detaching and upwards movement of bubbles of different diameters. At the beginning of the heating up process mainly small bubbles occur near the wall (Figure 8c). The wall boiling model releases bubbles having a diameter of about 1 mm. By the agglomerative effect of the cluster-force and using the principles of the GENTOP-concept it is possible to create continuous gas structures out of a dispersed gas phase (Figure 8d). After the wall boiling generation of small bubble sizes the domain is characterized by an increase of the mean bubble diameter due to the coalescence processes in the MUSIG-framework. When the mass transfer to the continuous gas begins and the volume fraction of GasC exceeds locally the threshold value $\alpha_{cg} > \alpha_{clust,min}$, here set to 0.5, the cluster-force agglomerates the continuous volume fraction until the complete coalescence replaces the dispersed gas fractions and large gas structures are resolved. They further coalesce to larger gas structures forming distorted cap-bubbles and larger slugs represented in the Figure 9. In this Figure the 3D isoline structures of GasD1 (blue), GAsD2 (green) and GasC (white) are shown at different stages of the boiling process.

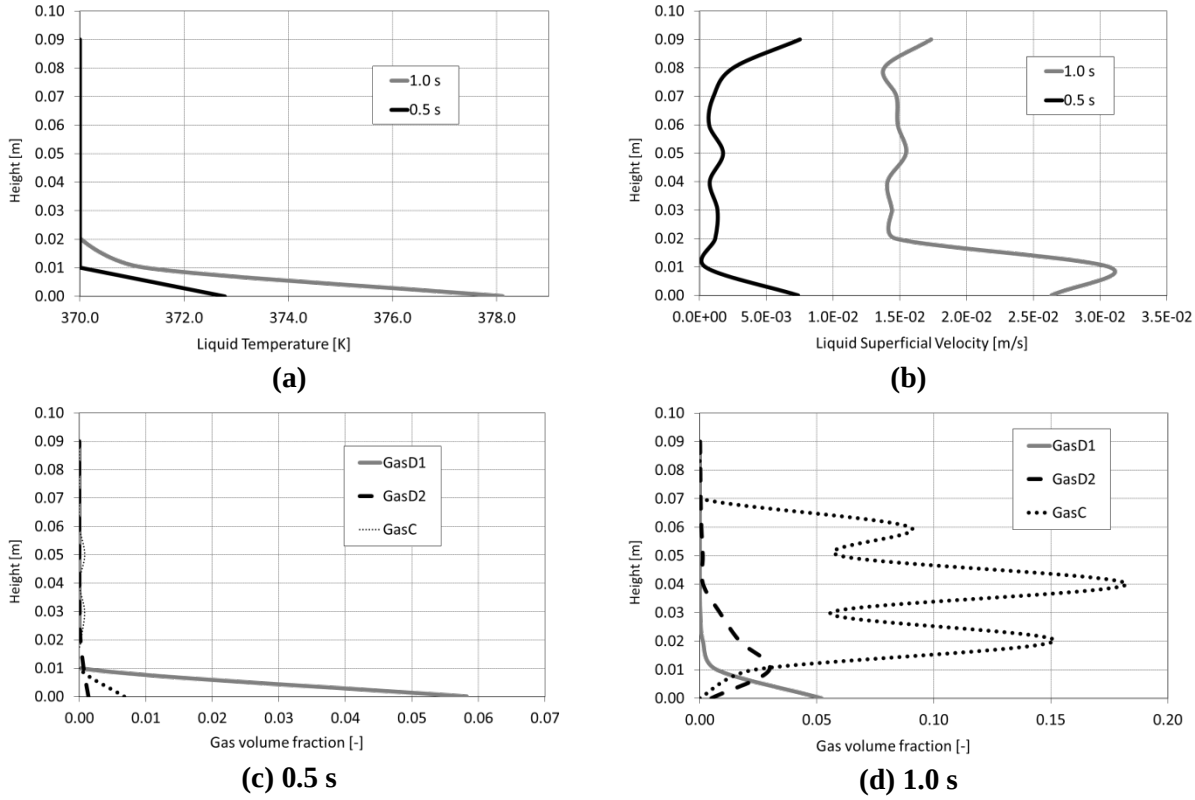

Figure 8: Horizontal averaged profiles for the liquid temperature (a), the liquid superficial velocity (b) and the gas volume fractions for different times (c, d).

In grid cells where the continuous gas volume fraction stays below the threshold value $\alpha_{cg} < \alpha_{clust,min}$ the gas is treated as a dispersed phase (GasD1 and GasD2) following the particle model formulations. At the later phase (Figure 9c) larger structures (white) of GasC are created. These structures are rising towards the surface of the pool. Close observation of the GasD and GasC/Liquid interface show that different flow regimes can be found in the simulation. The bubble flow regime occurs at relatively low gas flow rates (Figure 9a and 9b), for which the gas phase appears in the form of small bubbles in the lower part of the pipe. Later bubbly–slug flow is characterized by the presence of relatively large cap-shaped bubbles, which occupy nearly the entire pool and flow alongside smaller bubbles (Figure 9c and 9d).

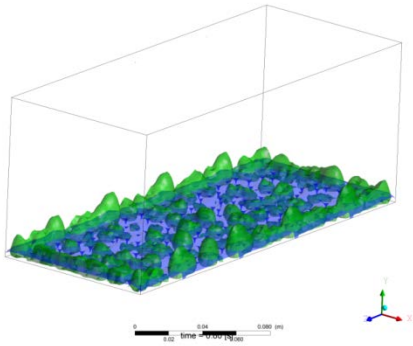

(a) Snapshot at 0.8 s after start of boiling

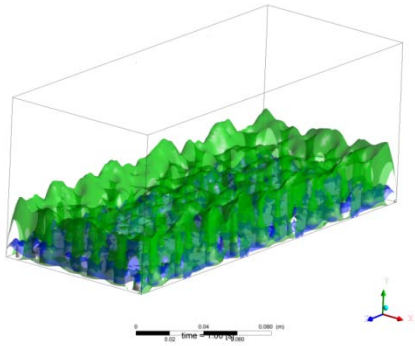

(b) Snapshot at 1.0 s after start of boiling

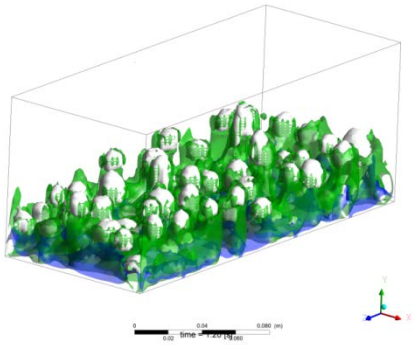

(c) Snapshot at 1.2 s after start of boiling

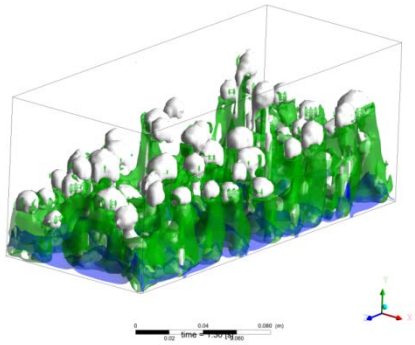

(d) Snapshot at 1.3 s after start of boiling

Figure 9: 3D isoline structures of GasD1 (blue), GAsD2 (green) and GasC (white)

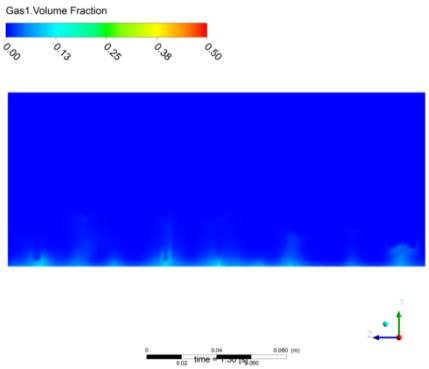

(a) GasD1 volume fraction [-]

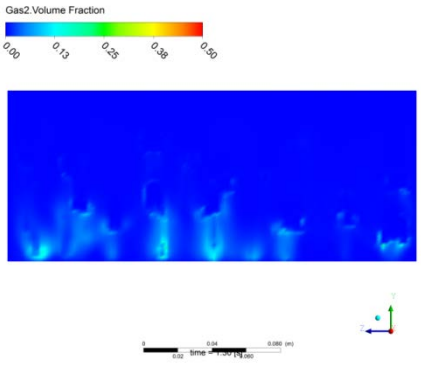

(b) GasD2 volume fraction [-]

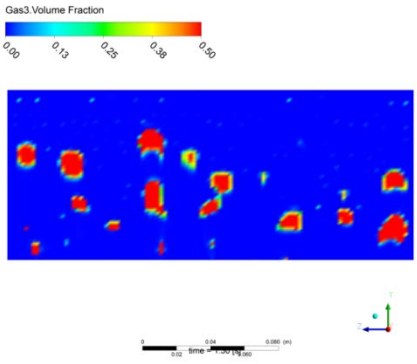

(c) GasC volume fraction [-]

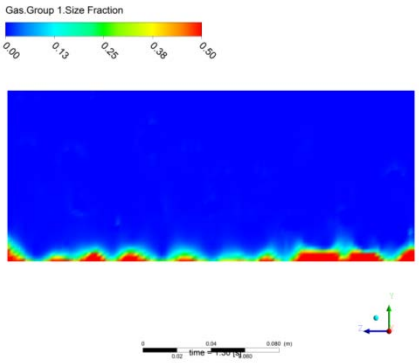

(d) Gas size group 1 size fraction (small bubbles) [-]

Figure 10: Snapshots of GENTOP model in the mid plane (y,z) outputs at 1.3 s

Figure 10 shows the snapshots of the GENTOP model in the pool mid plane (y,z) outputs at 1.3 s. In this Figure the GasD1/GasD2 and GasC volume fractions are shown (Figure 10 a-c). In addition one can see the Gas Size group 1 Size fraction (smallest bubbles) generated at the heated wall (Figure 10d).

Figure 11 represents essential GENTOP parameters in the mid plane (y,z) of the pool at 1.3 s. The cluster force is accting stabilizing the interface between GasC and Liquid (Figure 11a). From the other side the surface tension force is acting in contradiction to the cluster force (Figure 11b). Figure 11c shows the liquid temperature. The temperature is not equally distributed. Hot plumes arising randomly also dependening on the velocity of rising bubbles and larger structures. Figure 11d shows the liquid superficial velocity. The largest velocities occure behind the rising of the larger cap bubbles and structures.

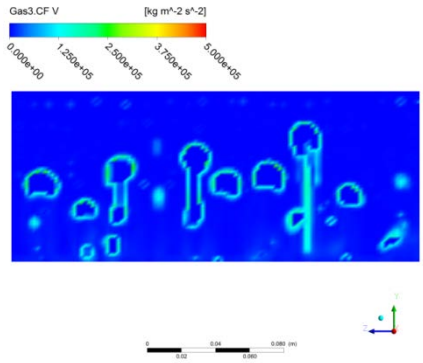

(a) Cluster force [kg m^{-2}s^{-2}]

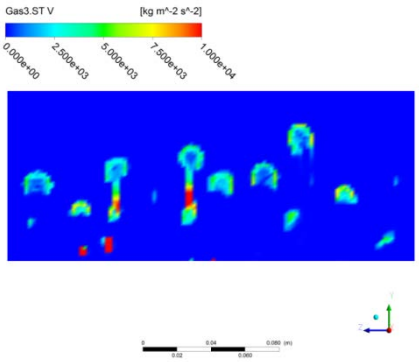

(b) Surface tension [kg m^{-2}s^{-2}]

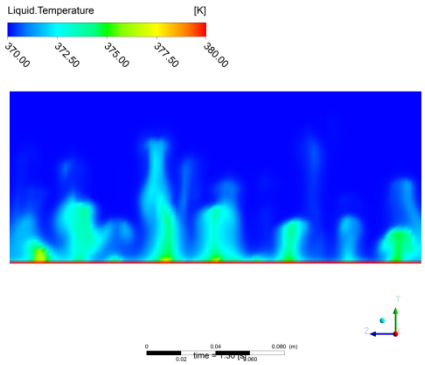

(c) Liquid temperature [K]

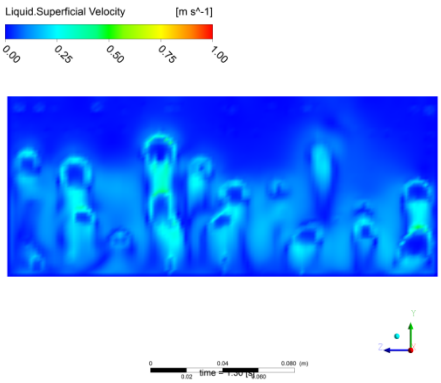

(d) Liquid superficial velocity [m/s]

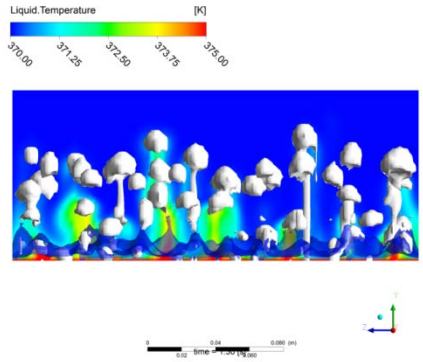

(e) Liquid temperature and 3D structures of GasD1 and GasC [K]

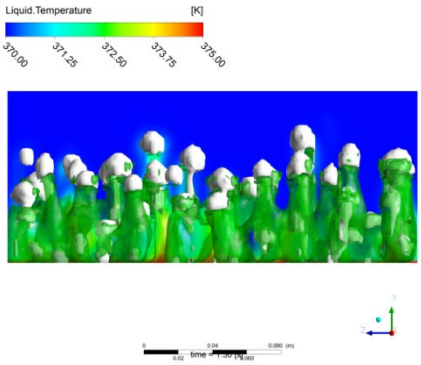

(f) Liquid temperature and 3D structures of GasD2 and GasC [K]

Figure 11: Snapshots of GENTOP model outputs in the mid plane (y,z) at 1.3 s

In Figure 11e the liquid temperature and the 3D structures (isolines) of GasD1 (blue) and GasC (white) are shown, while for clarity in Figure 11f the liquid temperature and the 3D structures (isolines) of GasD2 (green) and GasC are displayed. While smaller bubbles are basically localized at the wall and then with increasing wall distance more ore less disappear (Figure 11e), Figure 11f clearly shows the wake of small to medium size bubbles following the larger structures.

In order to compare the GENTOP pool boiling results with similar experimental and numerical results from the literature the experiments from [7] were used for qualitative comparison. In Figure 3 pool boiling experiment at the ISNPS-UNM Test Facility [7] are shown.

It is not straightforward to compare these pictures (Figure 3) to the numerical snapshots from Figure 9, since the boundary conditions are different between the experiments and the simulation. Qualitatively at least, the computed shapes of the disoriented cap bubbles and the slugs and those observed in the experiment are close. However, compared to the work of Sato and Niceno [24], where they simulated a series of pool boiling simulations using an interface tracking method, the GENTOP attempt modelling smaller bubble sizes as a disperse phase and larger structures resolved can significantly safe computational time.

SUMMARY AND FUTURE WORK

The GENTOP concept, which allows dealing with configurations involving dispersed and continuous interfacial structures, was coupled with a wall boiling model and extended to consider heat and mass transfer between gas and liquid in the bulk. New model aspects of GENTOP were implemented and tested. Starting with a sub-cooled liquid in a pool, bubbles (boiling) start to appear as soon as the liquid reaches its saturation temperature. Since, the temperature of bottom wall is above the saturation temperature of the liquid, bubbles start to depart and to grow fast. The macroscale simulation of the transitions from small bubble to larger structures during boiling in a pool is now feasible.

REFERENCES

[1] Nukiyama, S., The Maximum and Minimum Values of the Heat Q, Transmitted from Metal to Boiling Under Atmospheric Pressure, *Inst Jul Heat Mass Transfer, Vol 9*, p 1419, 1934.

[2] Farber, F.A. and Scorah, R. L., Heat Transfer to Water Boiling Under Pressure, Transaction ASME, Vol 79, p 369, 1948.

[3] Kreith, Bohn, "Principles of Heat Transfer", West Pub. Co., 1993

[4] Höhne, T.; Krepper, E.; Lucas, D.; Montoya, G., CFD-Simulation of boiling in a heated pipe including flow pattern transitions using the GENTOP concept, Nuclear Engineering and Design 322(2017), 165-176

[5] Hänsch, S., et al., A multi-field two-fluid concept for transitions between different scales of interfacial structures. International Journal of Multiphase Flow, 2012. 47: p. 171-182.

[6] Hänsch, S.; Lucas, D.; Höhne, T.; Krepper, E., Application of a new concept for multi-scale interfacial structures to the dam-break case with an obstacle, Nuclear Engineering and Design 279(2014), 171-181.

[7] http://isnps.unm.edu/research/facilities/

[8] Montoya, G., et al. Analysis and Applications of a Generalized Multi-Field Two-Fluid Approach for Treatment of Multi-Scale Interfacial Structures in High Void Fraction Regimes. in Proc. Int. Congress on Adv. on Nucl. Power Plants. ICAPP2014-14230, USA. 2014.

[9] Krepper, E., et al., The inhomogeneous MUSIG model for the simulation of poly-dispersed flows. Nuclear Engineering and Design, 2008. 238(7): p. 1690-1702.

[10] Höhne, T.; Porombka, P., Modelling horizontal two-phase flows using generalized models, Annals of Nuclear Energy 111(2018), 311-316

[11] Rzehak, R. & Krepper, E. CFD modeling of bubble-induced turbulence. International Journal of Multiphase Flow, 2013, 55, 138-155

[12] Rzehak, R.; Ziegenhein, T.; Liao, Y.; Kriebitzsch, S.; Krepper, E.; Lucas, D., Baseline model for simulation of bubbly flows, Chemical Engineering & Technology 38(2015), 19-72

[13] Ishii, M.; Zuber, N. “Drag Coefficient and Relative Velocity in Bubbly, Droplet or Particle Flows”. AIChE J., 25: 843-855 (1979).
[14] Tomiyama, A.; Sakoda, K.; Hayashi, K.; Sou, A.; Shimada, N.; Hosokawa, S., 2006. Modeling and Hybrid Simulation of Bubbly Flow. Multiphase Sci. Tech., 18(1), 73-110.
[15] Burns, A.D., et al. The Favre averaged drag model for turbulent dispersion in Eulerian multi-phase flows. in 5th international conference on multiphase flow, ICMF. 2004.
[16] Hosokawa, S., Tomiyama, A., Misaki, S., & Hamada, T. (2002). Lateral Migration of Single Bubbles Due to the Presence of Wall. In Proc. ASME Joint U.S.-European Fluids Engineering Division Conference (FEDSM2002), Montreal, Quebec, Canada (Vol. ASME Conf. Proc. 2002 Vol. 1: Fora, Parts A and B , 855).
[17] Ranz, W. and W. Marshall, Evaporation from drops. Chem. Eng. Prog, 1952. 48(3): p. 141-146
[18] Hughes, E. D., Duffey, R. B. “Direct contact condensation and momentum-transfer in turbulent separated flows”, International Journal of Multiphase flow 17, 599-619. (1991).
[19] Kurul, N. and M. Podowski. On the modeling of multidimensional effects in boiling channels. in ANS Proceeding of the 27th National Heat Transfer Conference. 1991.
[20] Krepper, E.; Rzehak, R.; Lifante, C.; Frank, T. 2013. CFD for subcooled flow boiling: Coupling wall boiling and population balance models, Nuclear Engineering and Design 255, 330-346
[21] Krepper and W. Ding, Review of Subcooled Boiling Flow Models, Handbook of Multiphase Flow Science and Technology, Yeoh G.H. (Ed.), Springer Singapore (2017), DOI: 10.1007/978-981-4585-86-6
[22] Luo, H. and H.F. Svendsen, Theoretical model for drop and bubble breakup in turbulent dispersions. AIChE Journal-American Institute of Chemical Engineers, 1996. 42(5): p. 1225-1233.
[23] Prince, M.J. and H.W. Blanch, Bubble coalescence and break-up in air-sparged bubble columns. AIChE Journal, 1990. 36(10): p. 1485-1499.
[24] Y. Sato, B. Niceno,(2018), Pool boiling simulation using an interface tracking method: From nucleate boiling to film boiling regime through critical heat flux, International Journal of Heat and Mass Transfer 125 (2018) 876–890